Anisotropic thermoelectric effect and field-effect devices in epitaxial bismuthene on Si (111)

Anisotropic thermoelectric effect and field-effect devices in epitaxial bismuthene on Si (111)

Wen Zhong[1,#], Yu Zhao[2,#], Beibei Zhu[1,#], Jingjie Sha[2,*], Emily S. Walker[3], Seth Bank[3], Yunfei Chen[2,*], Deji Akinwande[3,*], Li Tao[1,*]

[1]School of Materials Science and Engineering, Jiangsu Key Laboratory of Advanced Metallic Materials, Southeast University, Nanjing, 211189, China. [2]School of Mechanical Engineering, Jiangsu Key Laboratory for Design and Manufacture of Micro-Nano Biomedical Instruments, Southeast University, Nanjing, 211189, China.

[3]Microelectronics Research Center, the University of Texas at Austin, Texas 78758, USA.

[#]These authors contributed equally.

*e-mail: tao@seu.edu.cn; deji@ece.utexas.edu; yunfeichen@seu.edu.cn; major212@seu.edu.cn

Abstract

This experimental study reveals intriguing thermoelectric effects and devices in epitaxial bismuthene, two-dimensional (2D) bismuth with thickness ≤ 30 nm, on Si (111). Bismuthene exhibits interesting anisotropic Seebeck coefficients varying 2-5 times along different crystal orientations, implying the existence of a puckered atomic structure like black phosphorus. An absolute value of Seebeck coefficient up to 237 μV/K sets a record for elemental Bi ever measured to the best of our knowledge. Electrical conductivity of bismuthene can reach up to 4.6×10^4 S/m, which is sensitive to thickness and magnetic field. Along with a desired low thermal conductivity ~ 1.97 W/m·K that is 20% of its bulk form, the first experimental zT value at room temperature for bismuthene was measured ~ 10^{-2}, which is much higher than many other VA Xenes and comparable to its bulk compounds. Above results suggest a mixed buckled and puckered Bi atomic structure for epitaxial 2D bismuth on Si (111). Our work paves the way to explore potential applications, such as heat flux sensor, energy converting devices and so on for bismuthene.

Keywords: bismuthene, thermoelectric effect, anisotropic, 2D materials, Xenes

1. Introduction

Initial investigations on semiconductor type black phosphorus suggest good prospects for electrical, thermal and optical applications [1, 2], which arouses increasing research interest into two-dimensional (2D) Xenes, mostly group IVA and VA elemental atomic sheets. Bismuth is a post transition metal with a high carrier mobility ~ 20,000 $cm^2/V \cdot s$ [3] due to small effective mass, low thermal conductivity ~ 10 $W/m \cdot K$ [4, 5] and its longer mean free path (MFP) for phonons than electrons. These properties make bismuth and its 2D form, bismuthene, promise in thermoelectric device applications. Despite the recent progresses [6, 7] on bismuthene synthesis and electrical characterization, there is a lack of experimental study on its thermoelectric properties.

Thermoelectric effect converts heat into electricity, which holds great promise to address energy demands as a sustainable power generator [8, 9]. The efficiency of conversion is determined by the dimensionless figure of merit (zT), as

$$zT = \frac{S^2\sigma}{k}T \qquad (1)$$

Where S stands for the Seebeck coefficient, σ denotes the electrical conductivity, $S^2\sigma$ is the power factor, k represents the thermal conductivity and T is the temperature. The interplay of these three parameters (S, σ, k) is the key challenge to achieve high zT, while 2D materials become a better fit. According to the Hicks and Dresselhaus theory [10-12], the density of states of 2D materials can significantly deviate from bulk case. As a result, the Seebeck coefficient can be enhanced by tuning the width of the 2D quantum well without decreasing the electrical conductivity much, due to the large asymmetry existing between hot and cold electrons[13]. Thus, not only can the calculated zT value of 2D materials be improved by doping level, but also it can be tuned by scaling down the dimension, which provides another degree of freedom to design and improves the thermoelectric property of 2D Xenes like bismuthene.

zT value of single crystal bulk bismuth was measured 1.8 [4] at room temperature, which is lower than that of bulk Bi_2Te_3-based derivatives, renowned as commercial mainstream thermoelectric materials. It is mainly due to the bulk bismuth's low absolute Seebeck coefficient (|S|) of ~ 80 μV/K [14], while Bi_2Te_3-based materials can reach 150-260 μV/K [15, 16]. The calculated value 342 μV/K was obtained by Wu *et al.* [17] using the first principles calculation and Boltzmann transport theory. Here, we

denote 2D as the thickness that is less than its MFP, which is about 30 nm for Bi according to theoretical calculation. However, when Cho *et al.* [18] and Das *et al.* [19] experimentally measured the |S| of 2D bismuth, which were on CdTe and glass substrates by MBE (Molecular beam epitaxy) and vacuum evaporation respectively. The values of |S| were only ~ 40 μV/K, which were smaller than that of bulk bismuth. It is believed that synthesis method, substrate selection and thickness are needed to be optimized. The electrical conductivity of bismuthene was also investigated. Cheng *et al*. [20] predicted the electrical conductivity of monolayer bismuth could be up to 10^8 S/m, which was two orders of magnitudes larger than that of the bulk [21]. Compared with the conventional external elemental doping or alloying technique, for example, when Te was alloyed with Bi, |S| of Bi was increased by ~ 25% while electrical conductivity was decreased by 45%. When Se or Cu was doped in Bi-based compound Bi_2Te_3, the |S| was increased by ~ 30% - 50% while electrical conductivity was decreased even by 70% [22, 23]. The approach to scaling down the thickness from bulk to 2D might be more promising in improving thermoelectric performance in bismuth, because electrical conductivity may not be sacrificed too much when |S| is improved. It is noted that when the thickness of bismuth thin film increases too much such as 100 nm or glass substrate is selected, the electrical conductivity is 10 times lower than that of bulk counterpart [14, 19], suggesting process optimization is also needed as that in |S|. Thermal conductivity of bismuthene has been rarely measured experimentally [24]. Cheng *et al.* [20] predicted the *zT* value of a single layer of bismuth could reach up to 2.4 at room temperature and reach a maximum of 4.1 at 500 K, which indicated that low-dimensional bismuth could yield better thermoelectric properties than bulk and became a great candidate for energy devices.

Apart from the lack of comprehensive study on the *zT* values of 2D bismuth, it remains unclear for a scientific question: how do the thickness and interface affect thermoelectric properties of bismuthene? Here, we disclose the effect of layer/thickness to the electrical and thermal transport of 2D bismuth. Our experimental work combines preparation, device integration and comprehensive characterizations of epitaxial bismuthene on Si (111), with the first experimentally measured *zT* values and other inspiring findings including anisotropic Seebeck coefficients much larger than its bulk form and magneto-transport behavior sensitive to small magnetic field down to 600 mT.

2. Experiment methods

The 2D bismuth samples are grown on Si (111) substrate via MBE in varied thickness, with detailed conditions available in a previous publication [25]. The phase and composition characterization of 2D bismuth are performed by X-ray Diffraction (XRD) with Cu Kα radiation, Raman with 532 nm green laser and scanning electron microscope - energy dispersive spectrometer (SEM-EDS), respectively. The surface roughness is examined by atomic force microscope (AFM).

2D bismuth FET device is fabricated by electron beam lithography (EBL) (ELPHY Quantum), as shown in Figure 1(a), followed by e-beam evaporation (VZS600Pro) and lift-off of 5/45 nm-thick Ti/Au electrodes that are used as source and drain electrodes. The length and width of bismuth channels can vary from 0.5 to 5 μm. Electrical characterization of 2D bismuth FETs is performed on a probe station (Cascade® EPS150) with semiconductor parameter analyzer (Keysight 2902) at room temperature. Then, a Seebeck coefficient device (PTM) is used to measure the Seebeck coefficient of 2D bismuth with temperature gradient along the specimen and cold end at room temperature (Figure 1(a)). In addition, the thermal conductivity of 2D bismuth is measured using the time-domain thermoreflectance (TDTR) method (Section I in Supplementary Information), which is a pump-probe optical technique seen in Figure 1(b). Finally, the Hall effect measurements of 2D bismuth are carried on Hall effect test (HET) system with van der Pauw method.

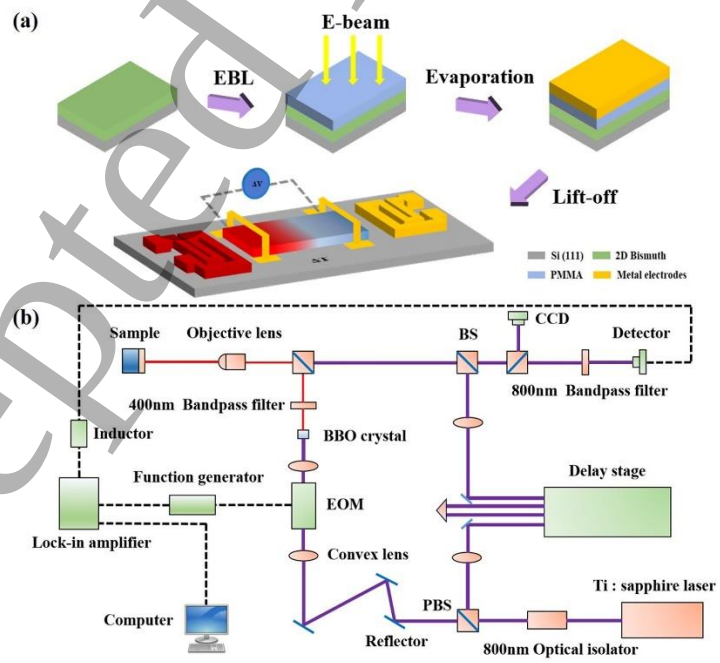

Figure 1. Experimental flow chart for 2D bismuth devices. (a) Electrical conductivity, Seebeck coefficient and **(b)** thermal conductivity measurements.

3. Results and discussion

A set of crystal structure, composition and surface characterization of 2D bismuth, prepared by MBE on Si (111) in this work exhibits high quality according to phase characterization, is carried out. There are two main kinds of lattices in 2D bismuth (Figure 2(a)): buckled and puckered, the latter of which is often more preferred when the thickness is beyond a critical point [26, 27]. Raman spectra (Figure 2(b)) consists of two distinct Raman vibration modes, around 71 cm^{-1} and 97 cm^{-1} that can be assigned to E_g and A_{1g} modes of bismuth (inset of Figure 2(b)), respectively [6, 28]. It is noted that, compared with bulk bismuth, there is a blue shift in E_g and A_{1g} Raman modes for 2D bismuth, which can be attributed to the phonon confinement effects due to lower dimensions [28] with possible alternation or transformation in crystal structure. Notably, there is no detectable Raman finger print of Bi_2O_3. XRD patterns (Section II in Supplementary Information) show high-level single crystallinity with exhibiting (001) peak only, indicating that 2D bismuth growth has preferred orientation along (001) direction (*PDF:85-1329*) It is worth mentioning that hexagonal (001) direction here is equivalent to (111) the rhombohedral coordinates for bismuthene crystal structure. The root mean square (RMS) roughness measures ~ 0.5 nm over 10 × 10 μm^2 area on 2D bismuth via AFM, as shown in Figure 2(c), which is sufficiently smooth for the later thermal conductivity measurement. The SEM image (Section II in Supplementary Information) and its attached EDS image (Figure 2(d)) as cross-references, which imply a good uniformity of 2D bismuth surface.

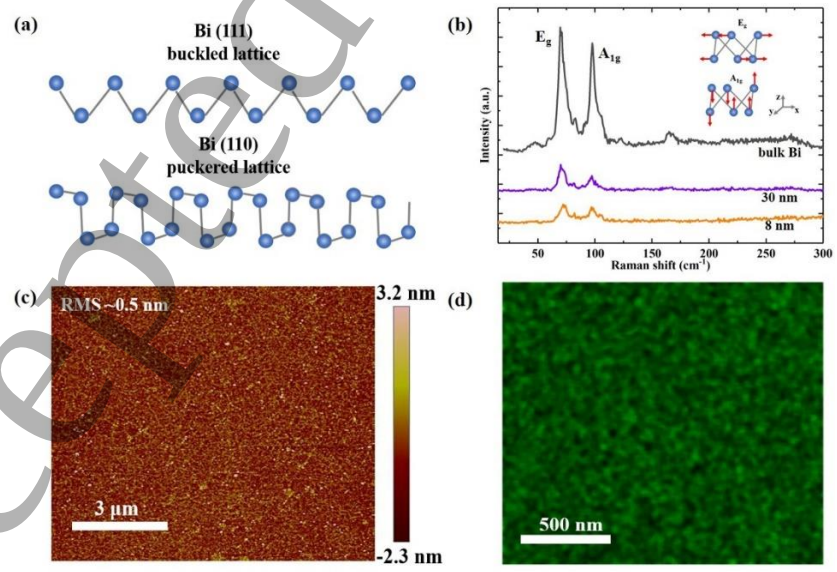

Figure 2. The structure, composition and surface roughness characterizations of 2D bismuth. (a) The lattice of 2D Bi. **(b)** Raman spectra, the inset image shows the vibration modes of bismuth. **(c)** AFM and **(d)** SEM with EDS mapping on Bi element.

Seebeck coefficient is measured as electrical potential difference across temperature gradients, which are associated with electron and phonon behavior. In 2D materials, the electronic states are distributed in a quantized manner, resulting in broadening band gap and increasing Seebeck coefficient [2], when the thickness decreases to a critical point based on quantum confinement effect [10-12]. Measured Seebeck coefficients of our 2D bismuth can go up to -237 μV/K, which is 2-5 times higher than reported values on thin film [29] or bulk bismuth [4, 14]. To the best of our knowledge, this is the first experimental evidence to prove that scaling down to 2D scale can significantly enhance Seebeck coefficient of bismuth. Substrate coupling could also play a role in enhancing Seebeck coefficient of 2D bismuth on Si (111), as seen by Cho *et al.* [18] and Das *et al.* [19], only ~ 40 μV/K of bismuth thin film on CdTe or glass substrate that has different lattice mismatch and strain when compared with Si (111).

Interestingly, 2D bismuth demonstrates an anisotropic Seebeck coefficient, which depends on the orientations. For instance, the Seebeck coefficients measured along with the orientation 1, 2, 5 in Figure 3 are -237 μV/K, -136 μV/K, -112 μV/K, respectively, whereas the values in the orientation 3 and 4, decrease to -42 μV/K and -58 μV/K. The Seebeck coefficients of bulk bismuth in Figure 3 have no anisotropy. Such anisotropic Seebeck coefficient values have only been discovered on black phosphorus so far [30], giving lower Seebeck coefficient in zigzag direction than that of armchair direction [26] due to anisotropic effective mass along with different crystal orientations in puckered atomic structure [31]. Here, we recall the references [26, 27] predicting the transition of 2D bismuth layer structure from puckered to buckled at around 7ML (3ML is roughly 1 nm). For 2D bismuth thicker than 7ML, *i.e.* 4 nm, 8 nm and 30 nm in this work, it could have a mixture of puckered (bottom layers) and buckled (top layers) lattice (Figure 2(a)). Our experimental observation supports this theory that gives a reasonable explanation on why 2D bismuth exhibits anisotropic Seebeck coefficient but not obvious as seen in black phosphorus. The anisotropic Seebeck coefficient agrees with the single crystalline of our MBE bismuthene, whereas an isotropic property is observed on amorphous or polycrystalline 2D bismuth via physical vapor deposition (Section III in Supplementary Information). Recently, similar structure induced by magnetic and optical anisotropy has been revealed on other low dimensional materials like CrOCl [32].

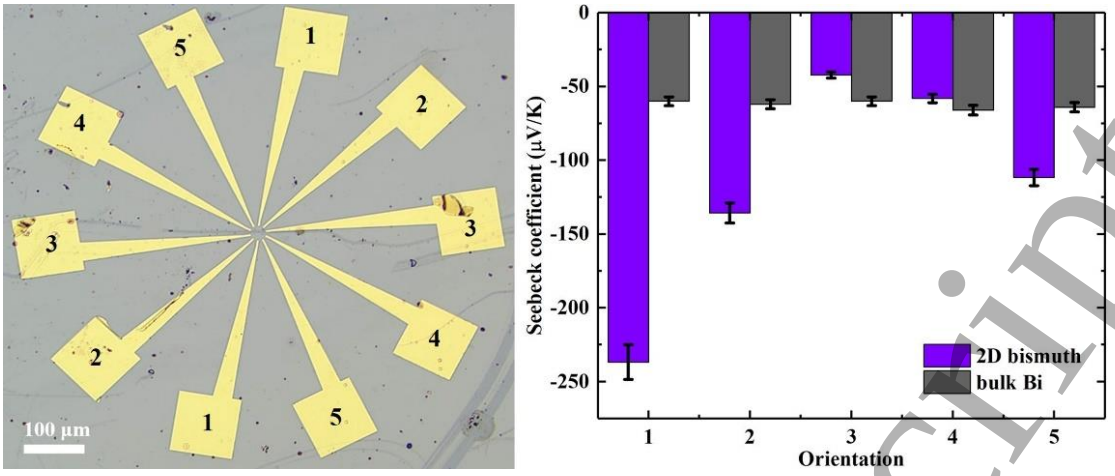

Figure 3. The Seebeck coefficients of 2D and bulk bismuth. The orientation-dependent Seebeck coefficients of 30 nm (each direction is ~ 36° to each other) and bulk bismuth.

Thermal conductivity of 2D bismuth is measured using the TDTR method (Section I in Supplementary Information). Based on the fitting results (Figure 4(a)), the thermal conductivity of 30-nm bismuth is 1.97 W/m·K at room temperature, which is consistent with the theoretical data 2 W/m·K [24] (Figure 4(b)). The value decreases by a factor of 5, when it is compared with the thermal conductivity of bulk bismuth (~ 10 W/m·K) [4, 33]. As is known to the phonon interface scattering theory [34, 35], when the scale of the material is reduced to 2D, the thermal conductivity of the material will be affected, especially when the size of the material is reduced to the same or smaller than the average phonon MFP of bulk, the phonon scattering effect is obviously enhanced. In this case, the phonon transport is partially ballistic and the effective phonon MFP is limited by the thickness of the material due to phonon-boundary scattering by phonon confinement effects, which is proved in shift of E_g and A_{1g} modes for 2D bismuth in Raman spectra (Figure 2(b)). Thus, our measured thermal conductivity of 8-nm bismuth reducing to 1.25 W/m·K proves the theory that boundary scattering of phonons reduces the thermal conductance, which is beneficial for thermoelectric performance.

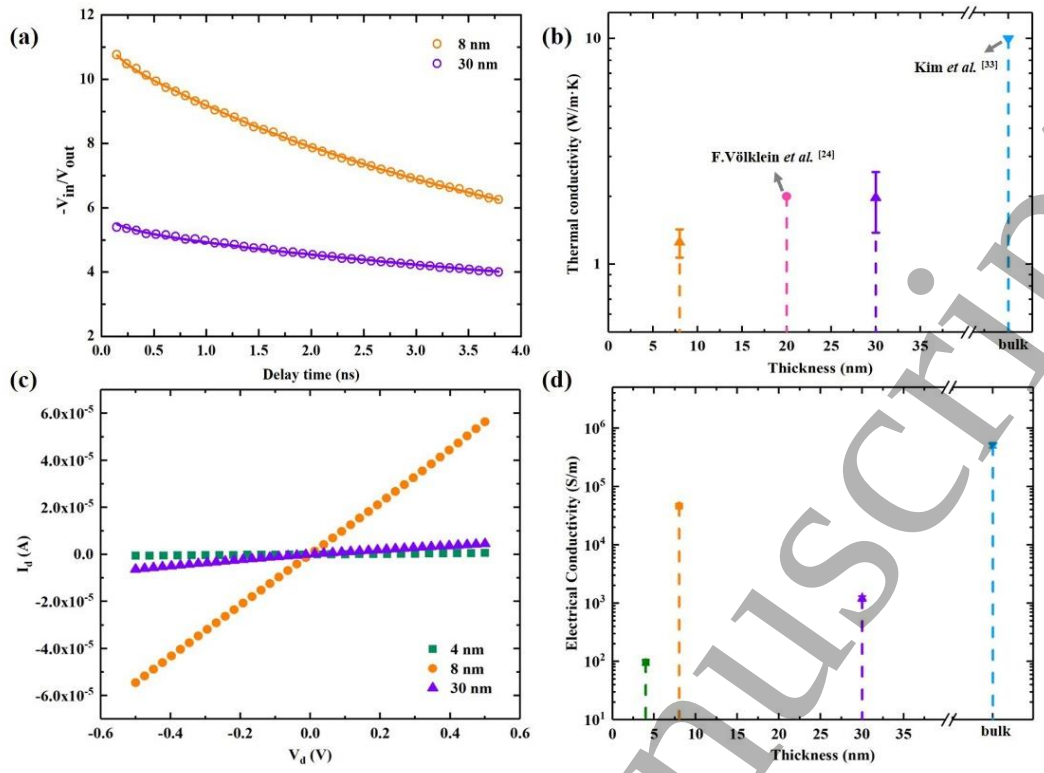

Figure 4. The thermal conductivity and electrical properties of 2D bismuth with different thickness. (a) The best fitting curve for 8-nm and 30-nm bismuth, at a modulation frequency of 1.72 MHz, a pump beam spot size of 12.0 μm and a probe spot size of 6.0 μm in the TDTR measurement, where the hollow circles and the solid lines denote the measured data and the thermal model fitting, respectively. **(b)** The thermal conductivity values of 2D and bulk bismuth. **(c)** The I_d-V_d curves of 2D bismuth. **(d)** The electrical conductivity values of 2D and bulk bismuth.

The effect of thickness on electrical conductivity is measured on 4, 8 and 30-nm bismuth FETs. Electrostatic measurements reveal a typical linear I_d-V_d curve, representing an ohmic contact between the metal electrodes and 2D bismuth (Figure 4(c)). The observed electrical conductivity σ of 2D bismuth runs from 1.2×10^2 to 4.6×10^4 S/m, which is 10 times lower than the bulk bismuth ~ 5.1×10^5 S/m [14]. The calculated power factor is in the region from 2.1×10^{-6} W/m·K^2 to 6.7×10^{-5} W/m·K^2, which is lower than that of bulk bismuth (~ 1.9×10^{-3} W/m·K^2). The results are out of our expectation that the electrical conductivity could not be decreased much when the Seebeck coefficient was increased by around 5 times (Figure 3). This can be attributed to the transition from bulk metal with zero band gap to semimetal-semiconductor for 2D bismuth with a small band gap ~ 70 meV possibly due to quantum confinement (Section IV in Supplementary Information). An oscillatory rather than monotone thickness dependence of the electrical conductivity is observed, implying that there is not only one optimized thickness for electrical and subsequent thermoelectronic

property of bismuthene. For example, the highest electrical conductivity ~ 46250 S/m (Figure 4(d)) occurs at the thickness 8 nm, while 4 nm or 30 nm both experienced a drop in electrical conductivity because of the reduction in carrier concentration and charge mobility that is verified in Hall effect measurements (Table 1). The decreased carrier concentration probably results from the change in the band overlap energy subject to quantum size effect [36], while charge mobility reducing due to strong coupling between electrons and holes [33]. When the thickness reaching 4 nm, the electrical conductivity dropped sharply (Figure 4(d)) owing to the decreased mobility from surface scattering. Such oscillation in electrical conductivity has also been observed in Bi nanowires and thin films [33] , indicating nonmonotone thickness-dependent charge transport behavior in low dimensional bismuth.

Table 1. Hall effect measurements of 2D and bulk bismuth at room temperature

Thickness	*Electrical conductivity (S/m)*	*Hall coefficient (cm^3/C)*	*Carrier concentration ($/cm^3$)*	*Mobility ($cm^2/V·s$)*
8 nm	892.9	36.3	1.7×10^{17}	322.3
30 nm	339.7	73.4	8.5×10^{16}	250.7
bulk	5.1×10^{5}	-0.7	8.7×10^{18}	3690.0

It is observed that the absolute values of electrical conductivity measured by Hall effect measurement are 1-2 orders of magnitude smaller than those measured by FETs (Table 1 and Figure 4(d)). This phenomenon can be attributed to the small 600 mT magnetic field, which could significantly affect the effective mass of charge carriers [37] and lead to the decreased electrical conductivity. It is interesting to observe that the 2D bismuth is switching from ***N-type*** (Figure 3) to ***P-type*** (Table 1), which is the same type in bismuth thin film recently synthesized by PLD [6], while bulk is consistent with ***N-type***. It is worth mentioning that for bulk bismuth, the magnetic field that can induce ***P-type*** charge carrier has to reach a high magnetic field 14 T [38]. Inspiringly, in our work it only needs a small magnetic field 600 mT for 2D bismuth to show similar effect, which indicates a highly sensitive B-field sensor application.

Based on the aforementioned Seebeck coefficient, electrical conductivity and thermal conductivity measurements, the calculated zT values of 2D bismuth vary from 10^{-3} to 10^{-2} (Table 2). To our best knowledge, this is the first report of zT value in single

crystalline 2D bismuth below 30 nm. The value is higher than those of pristine graphene and black phosphorus in certain crystal orientation [13, 39], comparable to bulk bismuth [14] 5.9×10^{-2} and its compounds used for thermoelectric applications. The room for further improvement in our work is to increase electrical conductivity (Figure 5). New developed growth techniques were applied in 2D bismuth in our present work. It is worth mentioning that the power factor of our 2D bismuth with the developed synthesis process can be up to 1.1×10^{-3} W/m·K^2 (Section V in Supplementary Information), which is due to the obtained electrical conductivity quite close to that of bulk bismuth and even higher than those of bulk Bi-based compounds (Figure 5). However, the advantage of high Seebeck coefficient in MBE samples is suppressed. Synthesis parameter's optimization is needed in the future. Another approach to increasing the electrical conductivity is suggested to scale down to thinner bismuthene, which can help decrease thermal conductivity at the same time (Figure 5). According to Hicks & Dresselhaus [10], the quantum confinement, which can produce exciting *zT* much larger than single digit, is supposed to be observed when the thickness of bismuth is smaller than 30 nm. Our on-going work is to identify an optimal thickness of 2D bismuth for an ideal thermoelectric performance [14, 15, 22, 23, 40, 41], which maintains Seebeck coefficient ~ 10^2 μV/K and thermal conductivity below 2 W/m·K in this work, while increasing electrical conductivity higher than 10^5 S/m.

Table 2. The thermoelectric properties of 2D and bulk bismuth

Form	*Carrier type*	*Electrical conductivity (S/m)*	*Thermal conductivity (W/m·K)*	*Seebeck coefficient (μV/K)*	*zT value*
2D bismuth	N or P	10^3-10^4	1.25-1.97	42-237	10^{-4}-10^{-2}
bulk	N	5.1×10^5	10 [4, 33]	-62	5.9×10^{-2}

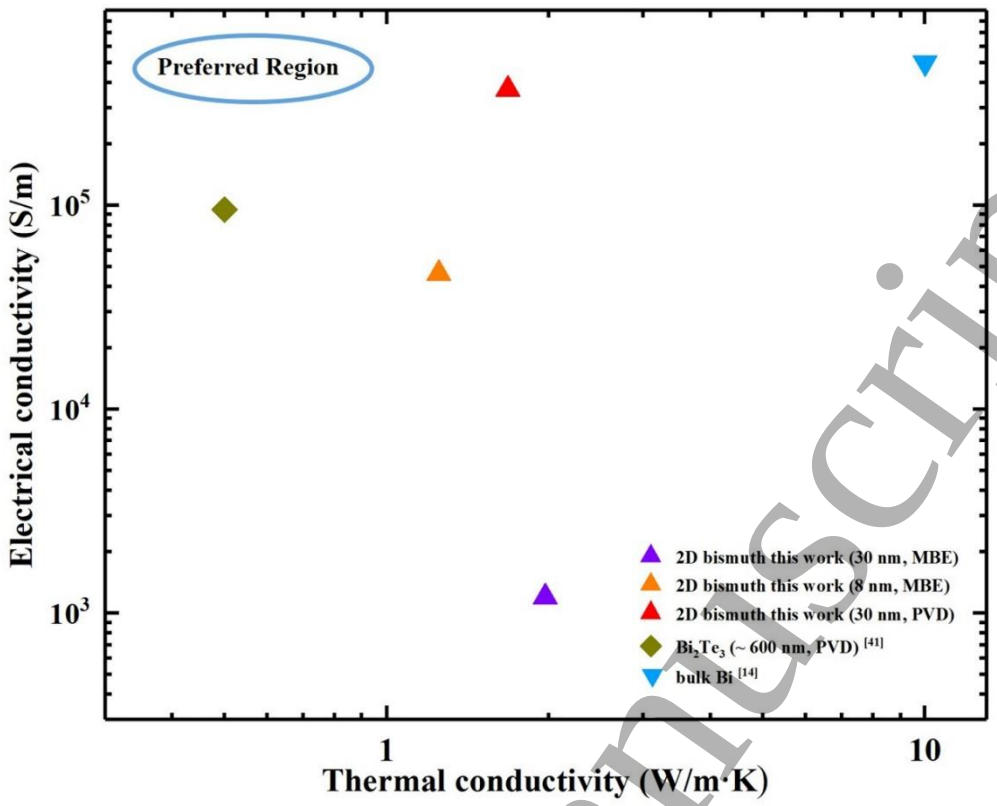

Figure 5. Roadmap of thermoelectric research work on 2D and thin film form of bismuth and its composites. Thermal conductivity of 2D bismuth is about one fifth of bulk Bi and electrical conductivity (30nm, PVD) is comparable to Bi_2Te_3 thin film and bulk Bi, suggesting that reducing thickness (number of layers) of bismuth is an effective strategy to improve thermoelectric performance without doping.

4. Conclusion

In summary, a comprehensive study about epitaxial 2D bismuth (≤ 30 nm) on Si (111) reveals its unique electric and thermal properties, such as anisotropic Seebeck coefficients possibly originated from its unique puckered-buckled mixture layered structure, and charge carrier type switching induced by small magnetic field. The electrical conductivity, Seebeck coefficient and thermal conductivity of 2D bismuth were measured up to 46250 S/m, -237 μV/K and as low as 1.25 W/m·K at room temperature, respectively. The *zT* value of 2D bismuth without optimization measures ~ 1.0×10^{-2} at room temperature, with further improvement on the way. This work pinpoints the thermoelectric anisotropy with the first experimental *zT* value measured on bismuthene. Our bismuthene device paves the way to explore potential innovative nanoelectronics, such as alternative energy device, heat flux and magnetic field sensors.

Acknowledgements

The authors acknowledge fruitful discussion with Professor Jiamin Xue at Shanghai University of Science and Technology and Professor Yufeng Hao at Nanjing University. L.T. acknowledges the support from National Natural Science Foundation of China (51602051), Jiangsu Province Innovation Talent Program, Jiangsu Province Six-Category Talent Program (DZXX-011). J.S. and Y. C. acknowledge the support from National Natural Science Foundation of China (51435003 and 51675101). S.B. acknowledges the support from National Science Foundation under NSF Award (DMR-1720595), and D.A. acknowledges the support from the Presidential Early Career Award for Scientists and Engineers (PECASE).

Author Information

B.Z. and L.T. conceived the idea and planned the experiment with W.Z. and Y.Z. E.W. performed the molecular beam epitaxy experiment under supervision of S.B and D.A. W.Z. and Y.Z. performed the electrical, thermal and Seebeck measurement experiment and data analysis under the supervision of L.T., J.S. and Y.C. W.Z, Y.Z. and B.Z wrote the manuscript with input from all authors.

Competing interests

The authors declare no competing interests.

References

1. X.Liu *et al.* 2020 Advances of 2D bismuth in energy sciences. *Chem Soc Rev*. **49**(1) 263-285.
2. M.Pumera *et al.* 2017 2D Monoelemental Arsenene, Antimonene, and Bismuthene: Beyond Black Phosphorus. *Adv Mater* **29**(21) 1605299.
3. D.L.Partin *et al.* 1988 Growth and characterization of epitaxial bismuth films. *Phys. Rev. B.* **38**(6) 3818-3824.
4. C.F.Gallo *et al.* 1963 Chandrasekhar, and P.H. Sutter, Transport Properties of Bismuth Single Crystals. *J. Appl. Phys.* **34**, 144-152.
5. H.K.Lyeo *et al.* 2006 Thermal conductance of interfaces between highly dissimilar materials. *Phys. Rev. B.* **73**, 144301.
6. Z.Yang *et al.* 2019 Centimeter‐scale growth of two‐dimensional layered high‐mobility bismuth films by pulsed laser deposition. *InfoMat* **1**, 98-107.
7. P.J.Kowalczyk *et al.* 2020 Realization of Symmetry-Enforced Two-Dimensional Dirac Fermions in Nonsymmorphic alpha-Bismuthene. *ACS Nano* **14**(2) 1888-1894.
8. D.W.Liu *et al.*2010 Fabrication and evaluation of microscale thermoelectric modules of Bi2Te3-based alloys. *J. Micromech. Microeng*. **20** 125031.

9. I.H.Kim *et al.*2000 $(Bi,Sb)_2(Te,Se)_3$-based thin film thermoelectric generators. *Mater. Lett.* **43** 221-224.
10. L.D.Hicks *et al.* 1993 Use of quantum ‐ well superlattices to obtain a high figure of merit from nonconventional thermoelectric materials. *Appl. Phys. Lett.* **63**, 3230-3232.
11. L.D.Hicks *et al.* 1993 Thermoelectric figure of merit of a one-dimensional conductor. *Phys. Rev. B.* **47** 16631-16634.
12. L.D.Hicks *et al.* 1993 Effect of quantum-well structures on the thermoelectric figure of merit. P*hys. Rev. B.* **47** 12727-12731.
13. J.Wu *et al.* 2018 Perspectives on Thermoelectricity in Layered and 2D Materials. *Adv. Electron. Mater.* **4** 1800248.
14. C.N.Liao *et al.* 2005 Thermoelectric characterization of sputter-deposited Bi / Te bilayer thin films. *Journal of Vacuum Science & Technology A: Vacuum, Surfaces, and Films* **23** 559-563.
15. S.I.Kim *et al.* 2015 Thermoelectrics. Dense dislocation arrays embedded in grain boundaries for high-performance bulk thermoelectrics. *Science* **348**, 109-14.
16. D.U. Yong *et al.* 2010 Preparation and Properties of Bi_2Te_3/Bi_2Se_3 Thermoelectric Nanocomposite Materials. *Journal of Materials Science &Engineering* 124.
17. C.Y.Wu *et al.* 2019 Influence of internal displacement on band structure, phase transition, and thermoelectric properties of bismuth. *J. Mater. Sci.* **54** 6347-6360.
18. S. Cho *et al.* 1997 Thermoelectric power of MBE grown Bi thin films and Bi/CdTe superlattices on CdTe substrates. *Solid State Commun.* **102** 673-676.
19. V.D.Das *et al.* 1987 Size and temperature effects on the Seebeck coefficient of thin bismuth films. *Phys. Rev. B.* **35** 5990-5996.
20. L.Cheng *et al.* 2013 Thermoelectric Properties of a Monolayer Bismuth. *J. Phys. Chem. C* **118** 904-910.
21. T.Arisaka *et al.* 2018 Investigation of carrier scattering process in polycrystalline bulk bismuth at 300 K. *J. Appl. Phys.* **123**(23) 235107.
22. A.Soni *et al.* 2012 Enhanced thermoelectric properties of solution grown Bi2Te(3-x)Se(x) nanoplatelet composites. *Nano Lett.* **12** 1203-9.
23. Q.Lognoné *et al.* 2014 Reactivity, stability and thermoelectric properties of n-Bi_2Te_3 doped with different copper amounts. *J. Alloys Compd.* **610** 1-5.
24. F.Völklein *et al.* 1984 A Method for the Measurement of Thermal Conductivity,Thermal Diffusivity, and Other Transport Coefficients of Thin Films. *Phys. Status Solidi.* **81** 585.
25. E.S.Walker *et al.* 2016 Large-Area Dry Transfer of Single-Crystalline Epitaxial Bismuth Thin Films. *Nano Lett.* **16** 6931-6938.
26. T.Nagao *et al.* 2004 Nanofilm Allotrope and Phase Transformation of Ultrathin Bi Film on Si(111)-7×7, *Phys. Rev. Lett.* **93** 105501.
27. Y.Lu *et al.* 2015 Topological properties determined by atomic buckling in self-assembled ultrathin Bi(110). *Nano Lett.* **15** 80-7.
28. N.Hussain *et al.* 2017 Ultrathin Bi Nanosheets with Superior Photoluminescence. *Small* **13** 1701349.
29. M.Inoue *et al.* 1975 Positive conductivity type in bismuth film. *Appl. Phys.* **8** 207-

209.
30. H.Liu *et al.* 2017 Variable range hopping electric and thermoelectric transport in anisotropic black phosphorus. *Appl. Phys. Lett.* **111** 102101.
31. H.Liu *et al.* 2014 Phosphorene: An Unexplored 2D Semiconductor with a High Hole Mobility. *ACS Nano* **8** 4033-4041.
32. T.Zhang *et al.* 2019 Magnetism and Optical Anisotropy in van der Waals Antiferromagnetic Insulator CrOCl. *ACS Nano* **13**(10) 11353-11362.
33. J.Kim *et al.* 2015 Diameter-dependent thermoelectric figure of merit in single-crystalline Bi nanowires. *Nanoscale* **7** 5053-9.
34. M.S.Dresselhaus *et al.* 2007 New Directions for Low-Dimensional Thermoelectric Materials. *Adv. Mater.* **19** 1043-1053.
35. G.Chen *et al.* 2004 Nanoscale Heat Transfer. *Encyclopedia of Nanoscience and Nanotechnology* **7** 429-459.
36. J.Kim *et al.* 2014 Quantum size effect on Shubnikov-de Haas oscillations in 100 nm diameter single-crystalline bismuth nanowire. *Appl. Phys. Lett.* **105**(12) 123107.
37. P.B.Alers *et al.* 1953 The Magnetoresistance of Bismuth Crystals at Low Temperatures. Physical Review, **91**(5) 1060-1065.
38. C.Uher *et al.* 1974 The Magneto-Seebeck Coefficient of Bismuth Single Crystals. *phys. stat. sol.* **63**(1) 163-169.
39. Q.Y.Li *et al.* 2019 Enhanced Thermoelectric Performance of As-Grown Suspended Graphene Nanoribbons. *ACS Nano* **13** 9182-9189.
40. G.Sun *et al.* 2015 Enhanced thermoelectric performance of n-type Bi2Se3 doped with Cu. *J. Alloys Compd.* **639** 9-14.
41. Q.Jin *et al.* 2019 Flexible layer-structured Bi2Te3 thermoelectric on a carbon nanotube scaffold. *Nat. Mater.* **18** 62-68.